

EVALUATION OF STATISTICAL MODEL FOR FUTURE PRECIPITATION AND TEMPERATURE IN DRAINAGE AREA OF JHELUM RIVER, PAKISTAN

Muhammad Imran Azam^{1,*}, Jiali Guo^{1,*}, Xiaotao Shi¹, Muhammad Yaseen², Altaeb Mohammed³, Haishen Lü⁵, Muhammad Tayyab¹, Zafar Hussain⁴ and Lingquan Dai¹

¹College of Hydraulic & Environmental Engineering, China Three Gorges University, Yichang 443002, China;

²Centre for Integrated Mountain Research (CIMR), University of the Punjab Lahore, Pakistan; ³College of Civil Engineering & Architecting, China Three Gorges University, Yichang, China; ⁴Water Resources Section, Ministry of Planning, Development & Special Initiatives, Islamabad, Pakistan; ⁵State Key Laboratory of Hydrology-Water Resources and Hydraulic Engineering, College of Hydrology and Water Resources, Hohai University, Nanjing, China

*Corresponding author's e-mail: jlguo1984@163.com; m.imranazam@hotmail.com

This study aims to the evaluation of an extensively used decision support tool “Statistical Down Scaling Model” (SDSM) for assessment of future variation in Precipitation (PPT), Temperature maximum (Tmax) and Temperature minimum (Tmin) of Jhelum River’s Drainage Area (JRDA), Pakistan. The current framework considered the partial correlation percentage (PRP) within 46.50%, 46.06%, 35.96%, and 21.97% to evaluate the effective predictors or the predictands. The R² values for both SDSM-M and SDSM-A models were calculated in scenarios 2.6, 4.5, and 8.5 RCPs under CIMP5 (CanESM-2). The R² precipitation values under all scenarios ranged between 82%-88% in SDSM-M. Whereas, R² for Tmin and Tmax was between 69%-71% and 68%-74%, respectively. For the SDSM-A model, precipitation ranged between 76.5%-80% for all scenarios, while Tmin and Tmax were found to be lying between 85%-92% and 89%-96%, respectively. Both models reflected seasonal and annual projected precipitation under RCPs 2.6, 4.5, and 8.5 from 13%-68%, 25%-69%, and 13%-71% in the 2020s-2080s, respectively. Tmin in annual models under RCP 2.6 decreased from -0.91 °C to -1.89 °C, -0.20 °C to -1.46 °C and -0.87 °C to -1.90 °C. The temperature under RCPs 2.6, 4.5, and 8.5 expressed a rise during the period 2020s-2080s from 0.04 °C to 3.75 °C, 1.02 °C to 2.62 °C, and 1.03 °C to 2.60 °C for the monthly model. Furthermore, an increasing trend was observed for Tmax from 0.01 °C to 4.18 °C, 0.01 °C to 4.49 °C and 0.12 °C to 3.90 °C in the period 2020s-2080s under RCPs 2.6, 4.5, and 8.5. The results revealed that the region will be generally warmer and wetter compared to the historical record. SDSM-A exhibited normal variation for the observed data compared to SDSM-M. It was concluded that the SDSM-A provided good results for average seasonal and annual temperatures (Tmax and Tmin). The results predicted the occurrence of more extreme events in JRDA during the 21st century. This study will be useful for water resources under different climatic conditions.

Keywords: SDSM-M (Monthly Statistical downscaling Model), JRDA (Jhelum River Drainage Area), SDSM-A (Annual Statistical downscaling Model), PRECIS (Providing Regional Climates for Impacts Studies), CanESM2 (Canadian the Second Generation Earth System Model), GCMs (Global Circulation Models), RCMs (Regional Climate Models)

INTRODUCTION

Climate change is gradually becoming complex around the globe. Whereas, from the hydrological perspective, the major effects of climate change are the rising sea levels due to the increase in temperature and amplification in the frequency and intensity of extreme events (IPCC, 2013). The increased emission of greenhouse gases in the environment resulting from human activities is the prime cause of global warming (Huang *et al.*, 2011; Chu *et al.*, 2010). The present rise in the global temperature may affect the hydrometeorological cycle, resource base, public health, commercial and domestic water demand (Huang *et al.*, 2011). Global warming is also apprehended to give rise to extreme climatic events, including hurricanes, heavy floods, and sultriness (Masson *et al.*, 2014). The average temperature had increased by 0.74 °C from 1906

to 2005, and a significant increase of 0.13 °C per decade has been recorded over the last 50 years. Therefore, for the sake of studying climatic variations, Global Circulation Models (GCMs) have been developed, which serve as the main source for providing information on climate change at regional and global levels (IPCC, 2007).

Whereas, Bias correction is a major concern regarding the accuracy of data acquired from GCMs. Bias Correction generate climate predictions at the local scale for impact studies such as crop and hydrology simulations (Su *et al.* 2016; Liu *et al.* 2017). Furthermore, several models have been developed for future data based on stochastic and regression methods. Statistical Down Scaling Model (SDSM) is frequently employed for downscaling by integrating regression as well as stochastic weather creators (Wilby *et al.*, 2002). Similarly, dynamic and statistical downscaling

methods were observed the level of bias for a yearly cycle in the data (Su *et al.*, 2017) and also found that the causes of variation in the weather of Auckland due to the disparity between climate model simulations and climate processes (Lowry *et al.*, 2017). All the GCMs predicted a thorough rainfall behavior in the Lucas Creek catchment area, and these GCMs can be categorized as a misty GCM related to the Weihe River catchment, China (Akhter *et al.*, 2008). Moreover, different combinations may assess the confidence limits, as suggested in the projected climate changes (Borges *et al.*, 2017). For patterns within the data, the records were verified to meet the necessities of the MK and SR tests for trends within the data of certain sites. Sen's slope method is employed to realize the slope scale in the record (Zaman *et al.*, 2017; Zaman *et al.*, 2016). Studies showed that annual precipitation (PPT) levels over the Midwest may increase for all RCP 8.5 models by the 2080s. However, the changes found prominent in winter (DJF) and spring (MAM). In contrast, mean changes in summer (JJA) and fall (SON) are relatively small (Byun and Hamlet, 2018).

RCMs were also used in a study to determine the impact of regional climate and to downscale the average precipitation and air temperature for 2071-2100 in the upper mountainous area of Pakistan (Akhter *et al.*, 2008; Ashiq *et al.*, 2010). Similarly, many researchers had employed SDSM in their projects to downscale the temperature, precipitation, and evaporation data in different catchments (Azmat *et al.*, 2018; Borges *et al.*, 2017). On the other hand South Asian countries (e.g. India) also showed a trend towards a warmer climate, which is experiencing a rapid rise in minimum surface temperature, extreme heat, and cold events (Basha Ghouse, 2017).

There are two main downscaling approaches: (a) statistical downscaling, and (b) dynamic downscaling. The impact of climatic change in a catchment is commonly assessed by the downscaling and the GCM outputs were used as boundary conditions to derive a regional climate model (RCM) up to 5–50 km on a regional scale. This approach responds to different external forcings in physically consistent ways (Wilby, 2007). Whereas, Dynamic Downscaling only involves RCMs that appeal for parity scenarios such as inputs to minimize the climatic data for the concerned periods at high spatial resolution (Rummukanian, 2010). It often requires specific point climate projections to capture fine-scale climate variations, particularly in regions with complex topographic coastal or island locations and areas of highly heterogeneous land cover (Fowler *et al.*, 2007).

Global Circulation Models (GCMs) deduced global systems like Oceans and atmosphere for predicting the divergence and change in weather variables for different grades (Fowler *et al.*, 2007). Similarly, statistical downscaling is generally helpful to make the climatic record at the location level for flood studies. Furthermore, the statistical method caters to the local

level climatic variables (predictors) and large level climatic variables (predictors) (Wilby & Dawson, 2007).

The detailed review, as performed above, it reveals that very few research studies have been conducted so far in the Jhelum River Drainage Area (JRDA), Pakistan. In fact, throughout South Asia, a gap exists between the capabilities of climate models to predict future climate change and the information relevant for the environmental studies. Statistical downscaling models are commonly used to fill this gap.

There are mainly three sub-models: i. Monthly, ii. Seasonal and iii. Annual. However, in the previous studies (Huang *et al.*, 2011), only the monthly sub-model has been used to downscale the climatic variables. Although the research has been conducted in the Jhelum River basin in Pakistan using the DD approach and interpolation methods for downscaling temperature and precipitation, Akhter *et al.* (2008) reported that PRECIS (Providing REgional Climates for Impacts Studies) has several sources of uncertainty. Similarly, Ashiq *et al.* (2010) stated that methods of interpolation could not improve the systematic errors inherent in PRECIS. Moreover, the above-mentioned studies forecast the temperature and precipitation data for the period 2071-2100 and not for the entire century. The objectives of this research were (1) to determine the applicability of SDSM sub-model of SDSM for Precipitation, Tmax and Tmin in JRDA, (2) to assess the SDSM sub-models for monthly and annual timescales and (3) to predict the future climate changes under IPCC scenarios (RCPs 2.6, 4.5 and 8.5) for the 21st century. The bid was to find out the influence of climatic variation on the Jhelum River Drainage Area (JRDA) Pakistan.

Research Area: The drainage area of the Jhelum River is situated on the southern gradient of the Himalayas, between the 33 ° N to 35 ° 12'N latitude and the 73 ° 07' to 75 ° 40' East longitude. The total span of the study area is 33425 square kilometers (at the Mangla Reservoir). The Jhelum River originates from Verinag Spring situated between the Himalayan Mountains of Jammu and Kashmir and the Pir Panjal Mountains. The major tributaries of the Jhelum River are the Neelum and the Kunhar, which have confluence at Muzaffarabad and Kohala, respectively (Figure 1). The drainage area is located in the complex monsoon region, which witnesses intense summer rainfall and light winter rain as well as snow. However, due to winter snowfall, which is a big source of summer runoff, precipitation is mostly accumulated in the Jhelum drainage area.

MATERIALS AND METHODS

Data Collection: Observed weather data (1971-2012) for all stations were collected from the Water and Power Development Authority (WAPDA) Pakistan and Pakistan Meteorological Department (PMD). Table 1 describes the features of climatic stations of the Jhelum River drainage area in Pakistan. The 26 predictors of CanESM2 (The

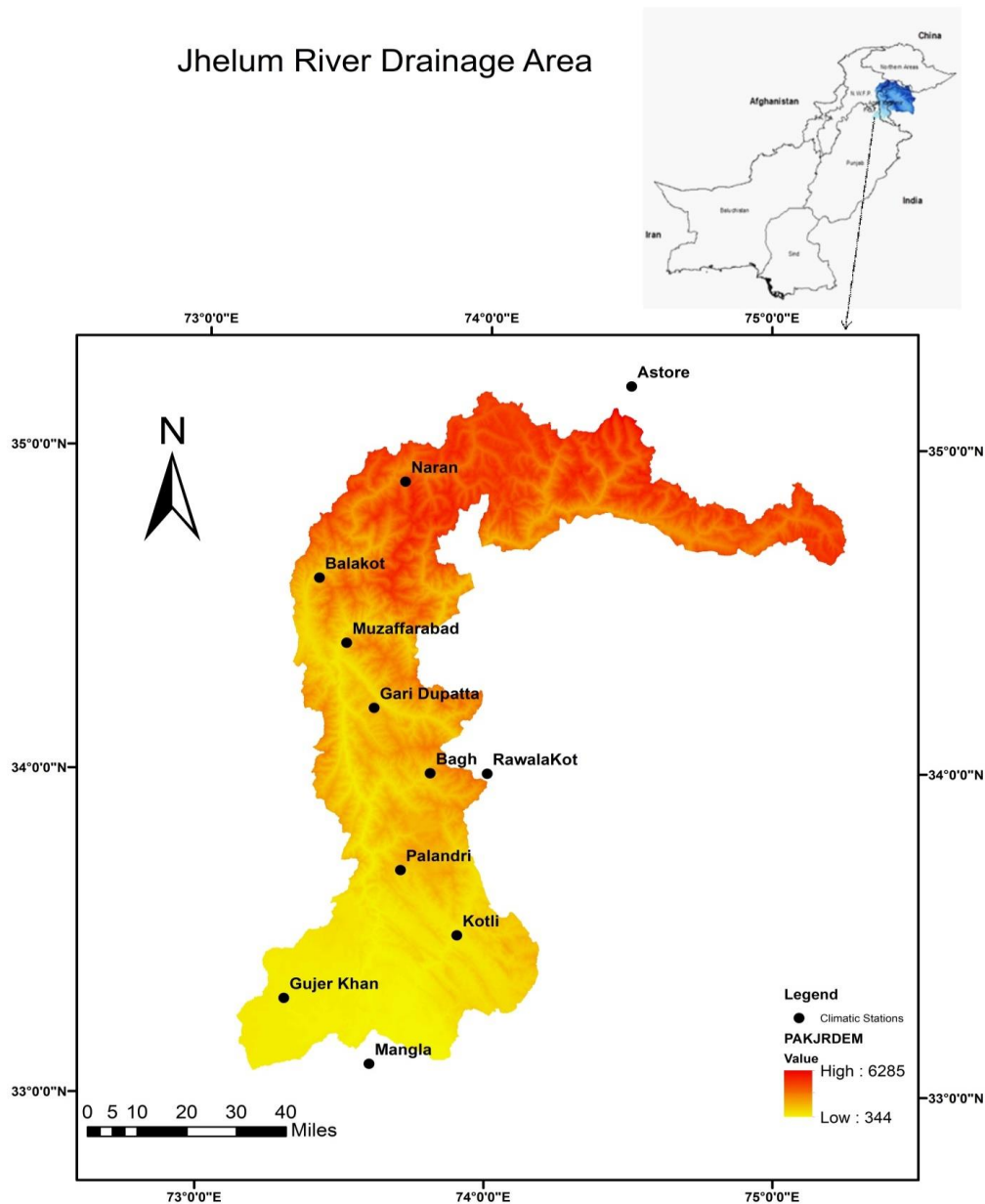


Figure 1. The Jhelum River Drainage area presenting weather stations and area in Pakistan.

2nd Generation Canadian Earth System Model) for CMIP5 (RCPs 2.6,4.5 &P8.5) were acquired from the Canadian Climate Centre. CanESM2 is a part of the Canadian Modeling Community's contribution to the IPCC, AR5. Main modules of the Earth System contain i) Atmospheric General Circulation Model which has triangular resolution T63 with a hybrid vertical domain in 35 layers, ii) Ocean GCM4 developed from the NCAR CSM Ocean Model and defined by 256x192 horizontal resolution and 40 vertical layers and iii) CanSim1 sea-ice model and Canadian Land Surface

Scheme (CLASS2.7). Global Gaussian reduced grid associated with spectral truncation T42 contains 128x64 grid cells in the longitude-latitude path.

The average monthly precipitation over the JRDA is shown in figure 2. As per Figure 2, the months of July and August showed the highest value of precipitation during the year due to Monsoon. Another monthly peak of precipitation was observed in February and March, as shown in Figure 2.

Figure: 3 Mean max. Monthly air Temperature over entire Jhelum River Drainage Area (JRDA)

Table 1. Weather station of the research and features.

Sr.	Location	Latitude (°)	Longitude (°)	Tmax. (°C)	Tmin. (°C)	AA.PPT (mm)
1	Bagh	34.0	73.8	12	22	746
2	Balakot	34.6	73.4	12	25	766
3	Gari Dupatta	34.2	73.6	12	26	922
4	Gujer Khan	33.3	73.3	15	29	503
5	Kotli	33.5	73.9	16	28	725
6	Muzaffarabad	34.4	73.5	14	28	712
7	Palandri	33.7	73.7	12	16	840
8	RawalaKot	34.0	74.0	9	21	745
9	Mangla	33.1	73.6	17	30	485
10	Naran	34.9	73.7	9	12	188
11	Astore	35.2	74.5	4	16	187

*Tmax= Max. Temperature; *Tmin=Mini. Temperature;

*AAPPT=Average Annual Precipitation

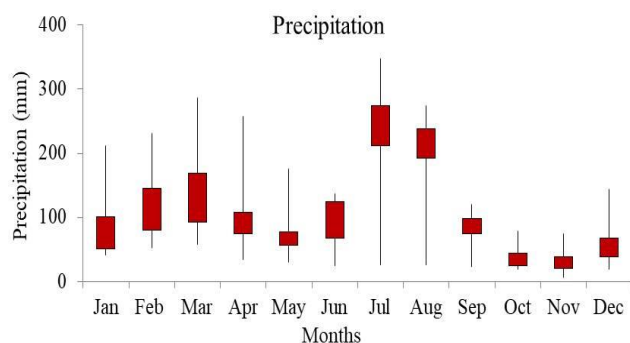


Figure 2. Mean Monthly precipitations over entire Jhelum River Drainage Area (JRDA).

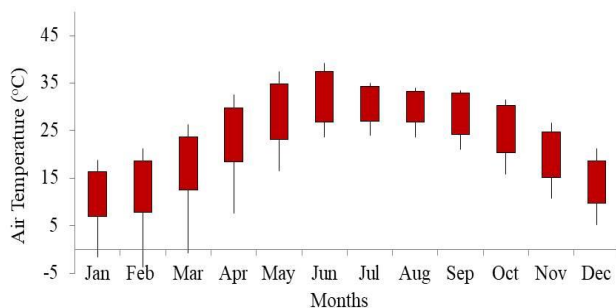


Figure3. Mean Monthly Tmax over entire Jhelum River Drainage Area (JRDA).

Mean monthly Max. Temperature has been presented in Fig. 3. The figure reveals the increase in Tmax during May and June. From July to September, monthly Tmax is almost at the same level. SDSM is made up of a stochastic weather generator (SWG) and multiple linear regression (MLR) compounds. Furthermore, multiple linear regressions develop a relationship between NCEP, large-scale variables, and local anesthetic scale variables as well as different regression factors (Liu *et al.*, 2009). In SDSM, some suitable predictors are selected through a multiple linear regression model utilizing the combination of the correlation matrix, partial

correlation, P value, histograms, and scatter plots. Multiple co-linearity must be considered during the selection of predictors. There are two main kinds of optimization techniques: (1) Ordinary Least Square (OLS) and (2) Dual Simplex (DS). Furthermore, for the determination of the relationship, predictors are selected by applying the combination of a correlated matrix, Partial correlation, P-value, histogram, and scatter plot. (Huang *et al.*, 2011). For the application of predictors, three kinds of sub-models can be used i.e. monthly, seasonal, and yearly to determine the statistical relationship between the local scalar variables and the large-scale atmospheric variables. Annual models derive the same type of regressions throughout the whole year, and the monthly sub-model presents the 12 regressions, offering a varied calibration parameter for every month. SDSM converts the records normally adored using the data in the regression equation (Khan *et al.*, 2006). Two kinds of daily time series, namely (1) daily historical site data and (2) NCEP daily predictors are used for developing SDSM. The outputs of this model are daily time series, which can be produced by forcing the NCEP or HadCM3 predictors (Huang *et al.* 2011).

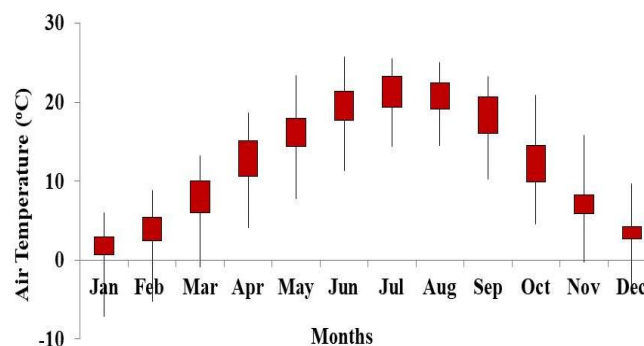


Figure 4. Mean monthly Tmin over entire Jhelum River Drainage area.

Selection of Predictors: In the present framework, the selection of predictors is of paramount importance. Therefore a systematic quantitative method is applied at each climatic station for the collection of large-scale variables.

The following steps were followed to select the predictors.

1. Firstly, a matrix of correlation was established between 26 NCEP predictors (Table 2) and predictants. Afterward, the twelve positive correlation coefficient predictors were selected from 26 and ranked in the descending order with the highest correlation between all predictors (Huang *et al.* 2011).
2. The absolute correlation coefficient was determined among the predictors and the predictands. P value was obtained by regression ingesting the remaining highly correlated predictors.
3. The predictors having a p value less than α (0.05) were removed, while the predictors having significant

correlation values (greater than 0.95) were selected to get rid of the multiple relations.

- Percent decrease in absolute partial correlation (PRP) regarding absolute correlation was found for every predictor by using the equation (1).

$$PRP = (P.r - R)/R \quad (1)$$

PRP= % reduction in partial correlation (PRP) with respect to absolute correlation, P.r= Partial correlation coefficient.R= Correlation coefficient among predictors and predictands.

- The Predictors having minimum PRP in partial correlation are selected as 2nd most appropriate predictor. This predictor may or may not have a strong relation with the first one (Table 3).
- From step 2 to 5 need to be repeated for the selection of 3rd or 4th predictors.

Table 2. List of used Predictors for Screening.

Sr.	Predictor	Description	Sr.	Predictor	Description
1	P_f	Surface airflow Strength	14	r500	500hPa relative humidity
2	P_u	Surface zonal velocity	15	p8_f	850hPaairflow strength
3	P_v	Surface meridional velocity	16	P8_u	850 hPa zonal velocity
4	P_z	Surface Vorticity	17	P8_v	850hPa meridional velocity
5	P_th	Surface Wind Direction	18	P8_z	850hPa vorticity
6	P_zh	Surface divergence	19	p8th	850hPa divergence
7	Rhum	Surface relative humidity	20	p8zh	850 hPa divergence
8	P5_f	500hPa airflow strength	21	r850	850hPa relative humidity
9	P5_u	500hPa zonal velocity	22	p500	500hPa geopotential Height
10	P5_v	500 hPa Meridional Velocity	23	p850	850hPa geopotential height
11	P5_z	500 hPa vorticity	24	temp	Mean Temp. at 2m
12	p5th	500hPa wind direction	25	shum	Surface specific humidity
13	p5zh	500hPa divergence	26	mslp	Mean sea level pressure

Table 3. screening of most effective predictors.

Sr.	Predictors	R	P.R (%)	P. R-R/R (%)
1	p1-f	0.227	8.4	35.96
2	p1-u	0.164	7.7	46.06
3	p1-v	0.200	9.5	46.50
4	p1-z	0.309	7.1	21.97
5	p5-f	0.127	0.0	-1.00
6	p5-u	0.209	0.0	-1.00
7	p5-v	0.382	6.7	16.55
8	p5-z	0.227	0.0	-1.00
9	p8-f	0.118	0.0	-1.00
10	p8-u	0.291	4.4	14.13
11	p8-v	0.300	0.0	-1.00
12	p8-z	0.182	0.3	0.65

*Substances in the bold are particular predictors

Calibration and Validation: SDSM Model 4.2.9 and CanESM2 were used to draw the future projections of the climatic data. The established monthly and yearly sub-models were labeled as SDSM-M and SDSM-A, respectively. For each station, individual models were developed for all predictand (Tmax, Tmin, and PPT) and the same predictors were used for the calibration of models. Therefore, the conditional sub-model was applied to Tmax and Tmin, and the unconditional sub-model was used for precipitation. After establishing the correlation between the models, the sub-models were simulated by using the observed PPT, Tmax, and Tmin from 1971-2001 under the RCPs 2.6, 4.5, and 8.5 of the IPCC scenarios. The results of the simulated models were compared with the observed data to determine the coefficient of determination (R²), Root Means Square Error (RMSE), Mean and standard deviation of the temperature and precipitation. These parameters indicate the accuracy of the model in the predicted data as well as how well the model predicts. Generally, the previous studies calculate the above-mentioned performance indicators at every weather station, and then the mean from all weather stations is determined. Whereas, our study firstly determined the monthly mean of the simulated data (Tmax, Tmin, and PPT) by both models utilizing the CIMP5 predictors. Afterward, it was compared graphically for the validation period.

RESULTS AND DISCUSSION

Screening of Predictors: We determined the 1st, 2nd and 3rd predictors for the PPT, Tmax and Tmin data as highlighted in table 3. It was identified that the Surface airflow strength (p_f) was the best predictor for both temperature and precipitation. Besides, there were two super predictors, surface meridional velocity (p_v) and surface zonal velocity (p_u) for almost all weather stations. Similarly, surface meridional velocity (p_v) was the main predictor in the lower area of the Himalayan of the Jhelum River Drainage Area (JRDA) Pakistan.

Calibration of Statistical Downscaling Model: PPT, Tmax, and Tmin were simulated for the period 1985-2001 by using both sub-models and compared with the observed data as shown in Table 4, 5. Although both models provided good results, SDSM-A illustrated better results than SDSM-M as revealed by the performance indicators. Regarding PPT, the monthly model performed better than an annual model with lower R² and higher values of RMSE than those of SDSM-M, for all IPCC scenarios. The standard deviation of SDSM-M simulation was lower compared to SDSM-A with 3.78, 3.76, 3.59 for all RCPs 2.6, 4.5 and 8.5, respectively. To validate both model datasets for all scenarios of the IPCC is generated from 2002-2012. Tables 4 and 5 show the results of SDSM-M and SDSM-A and the mean values which were worked out by applying the dataset for whole climatic stations. It was observed in the case of both temperatures (max & min) that the R² of SDSM-A is 85% to 96%, and RMSE for min temp

was from 3.25 °C to 3.45 °C. Similarly, RMSE for Tmax was from 7.96 °C to 8.20 °C lower than the SDSM-M model. In the case of precipitation, the R² and RMSE values were 82% to 88% as well as 380mm for 381.2mm, respectively, based on the SDSM-M model.

Table 4. Statistical comparison of observed and downscaled mean monthly Tmax, Tmin and Precipitation by SDSM-M Sub-models (2002-2012).

SDSM-M	Statistical Downscaling Model-Monthly			Standard Deviation (σ) mm
	R-Square	RMSE	Mean (μ) mm	
Precipitation				
Observed			104.51	13.81
RCP2.6	0.88	380.15	165.75	3.76
RCP4.5	0.86	380.00	161.25	3.87
RCP8.5	0.82	381.02	161.21	3.59
Min. Temp.				
Observed			11.01	1.13
RCP2.6	0.79	10.25	13.51	0.06
RCP4.5	0.69	10.20	13.45	0.06
RCP8.5	0.71	10.31	13.43	0.11
Max Temp.				
Observed			11.10	11.99
RCP2.6	0.74	9.77	24.10	0.06
RCP4.5	0.73	9.91	24.13	0.05
RCP8.5	0.68	9.78	24.11	0.06

Table 5. Statistical comparison of observed and downscale mean monthly Tmax, T min and Precipitation by SDSM-A Sub-models (2002-2012).

SDSM-A	Statistical Downscaling Model-Annually			Standard Deviation (σ) mm
	R-Square	RMSE	Mean (μ) mm	
Precipitation				
Observed			104.51	13.81
RCP2.6	0.80	459.52	174.63	4.63
RCP4.5	0.79	327.07	151.73	4.26
RCP8.5	0.76	376.70	154.99	9.54
Min. Temp.				
Observed			11.01	1.13
RCP2.6	0.85	3.45	11.72	0.11
RCP4.5	0.88	3.25	11.77	0.11
RCP8.5	0.92	3.35	11.73	0.10
Max Temp.				
Observed			11.10	11.99
RCP2.6	0.94	8.20	24.19	0.11
RCP4.5	0.89	7.96	21.74	0.22
RCP8.5	0.96	8.13	23.81	0.18

From table 4, 5, both models presented good results. However, the results with higher values of R² were better compared to the other model. SDSM-A performed much better compared to SDSM-M. Nevertheless, SDSM-M

produced a good result in the case of precipitation compared to SDSM-A for all scenarios of the IPCC. This indicated that SDSM-A is not capable to find the deviation in the observed record of precipitation. It is also evident from Table 4, 5 that most of the time, T max, T min, and rainfall predicted by the RCP4.5 and RCP8.5 produced better results. The RCPs 2.6, 4.5, and 8.5 were calibrated by both models using the dataset. However, the results of RCP 2.6 were also satisfactory.

Downscaling Project Precipitation and Temperature: SDSM-M and SDSM-A were used to simulate PPT, Tmax, and Tmin, in lieu of the future phases of the 2020s (2006-2020), 2050s (2021-2050), and 2080 (2051-2080) under the RCPs 2.6, 4.5, and 8.5 scenarios. The simulated monthly, seasonal and annual PPT, Tmax and Tmin data were equated with the baseline record (1971-2012) to find out the variations in the 2020s, 2050s, and 2080s in the study area and the results were presented in table 6, 7, 8, respectively.

Precipitation: Table 6 shows the variation in annual as well as seasonal mean precipitation for the 2020s, 2050s, and 2080s regarding the baseline record under the IPCC scenarios RCP 2.6, 4.5, and 8.5 from both models. Both models represented a mean yearly increment for historical data in the 2020s, 2050s, and 2080s for all scenarios. Under the RCP 2.6 scenarios, SDSM-A showed an increase in the average annual precipitation by 40% in 2020, 2050, and 2080 in the JRDA. Whereas, SDSM-M presented an increment of 36% under RCPs 4.5 and 8.5. For SDSM-A and SDSM-M, there was a slightly increasing trend with 35-36% and 31-40%, respectively. Rendering to the sub-models, all seasons expressed an increasing trend in the precipitation for the 2020s, 2050s, and 2080s.

Table 6. Future Changes in precipitation (%) with respect to baseline under RCP scenarios

	SDSM-A			SDSM-M		
	RCP2.6					
	2020	2050	2080	2020	2050	2080
Summer	15	15	15	33	34	34
Spring	41	41	43	56	55	55
Autumn	68	69	68	69	68	68
Winter	40	41	41	14	13	14
Annual	40	40	40	35	36	36
RCP4.5						
Summer	30	26	25	33	33	32
Spring	30	33	35	55	55	55
Autumn	60	58	58	69	68	68
Winter	26	25	26	16	14	16
Annual	36	35	36	35	35	35
RCP8.5						
Summer	25	14	13	33	33	34
Spring	41	33	34	57	57	58
Autumn	65	58	57	70	70	71
Winter	36	25	27	14	13	14
Annual	40	31	31	35	35	36

Both models during the autumn season showed an increasing trend of precipitation up to 70 by the end of this century for all scenarios of the IPCC. SDSM-A revealed an estimated increment of precipitation compared to SDSM-M. Spring and autumn exhibited changing behaviors of precipitation trends. **Minimum Temperature, Tmin:** Table 7 shows the change in the Tmin in the 2020s, 2050s, and 2080s with respect to a baseline record under RCPs 2.6, 4.5 and 8.5 scenarios from both SDSM-A and SDSM-M. The change in Tmin was projected by both models with different magnitude. In the case of the SDSM-A model, Tmin was found to be decreasing, for all IPCC scenarios in the 2020s, 2050s, 2080s during annual and seasonal. In winter for all scenarios, Tmin was increasing 1.26 °C to 1.29 °C for RCP 2.6, and RCP 4.5 also showed an upward trend from 1.54 °C to 1.88 °C, respectively. By using SDSM-M, the Tmin is increasing for all the IPCC scenarios. Under RCP 2.6, minimum temperature shows an increasing tendency by the start of the century with 3.75 °C. However, it expressed a gradual decline with 0.33 °C during the summer season. An almost similar situation was observed during the spring season with a 3.74 °C increment at the beginning of the century, and gradually declining till 0.11 °C by the end of the century. For the autumn season, temperature showed an increasing trend at 2.99 °C, but by the end, the temperature was on decreasing side with -0.10 °C. Similarly, for the other scenarios, the minimum temperature expressed an increasing trend over the entire JRDA in Pakistan.

Table 7. Future Changes in Tmin under RCP 2.6, 4.5, 8.5 Scenarios with two sub-models.

	SDSM-A			SDSM-M		
	RCP2.6			RCP2.6		
	2020	2050	2080	2020	2050	2080
Summer	-1.84	-1.84	-1.87	3.75	0.32	0.33
Spring	-1.02	-0.93	-0.77	3.74	0.04	0.11
Autumn	-0.87	-1.06	-1.36	2.99	0.04	-0.10
Winter	1.29	1.26	1.27	2.67	1.52	1.49
Annual	-0.91	-0.95	-0.98	3.04	0.21	0.20
	RCP4.5			RCP4.5		
Summer	-1.18	-1.46	-1.46	1.03	1.02	1.04
Spring	-0.35	-0.63	-0.37	1.18	1.19	1.28
Autumn	-0.20	-0.72	-1.02	1.18	1.12	0.98
Winter	1.88	1.54	1.60	2.63	2.62	2.62
Annual	-0.28	-0.60	-0.59	1.21	1.19	1.19
	RCP8.5			RCP8.5		
Summer	-1.85	-1.87	-1.90	1.03	1.06	1.09
Spring	-1.05	-0.87	-0.58	1.19	1.23	1.29
Autumn	-0.87	-1.11	-1.36	1.21	1.17	1.02
Winter	1.30	1.14	1.12	2.66	2.60	2.55
Annual	-0.92	-0.97	-0.97	1.22	1.23	1.21

Table 8 shows the change in the Tmax in the 2020s, 2050s, and 2080s with respect to a baseline record under RCPs 2.6, 4.5, and 8.5 scenarios from both models. Both models showed incremental changes for baseline in the 2020s, 2050s, and

2080s except for RCP 2.6 in SDSM-M, which showed a decrease in Tmax during all seasons. In summer, temperature expressed a decreasing trend from -7.07 °C in the 2020s and -4.19 °C by the end of the 21st century. For the spring, autumn and winter temperature revealed a decrease at the start of the century with -7.55 °C, -9.57 °C, and -7.49 °C in the 2020s, respectively, but in the 2080s temperature turned its trend towards increase with 2.38 °C, 0.22 °C, and 5.62 °C respectively. Similarly, for SDSM-A during autumn, the temperature expressed an increase by 0.37 °C in the 2020s and decrease by -0.01 °C in the 2080s. For RCP 4.5 in SDSM-A during spring, the temperature showed an increase by 4.60, 4.51, and 4.49 in the 2020s, 2050s, and 2080s, respectively. For annual analysis temperature displayed, decrease -1.18 °C, -1.30 °C and -1.42 °C in 2020s, 2050s and 2080s respectively. For RCP 8.5, the temperature showed an increase of 0.12 °C to 3.19 °C in the SDSM-A model and SDSM-M from 0.05 °C to 3.97 °C.

Table 8. Future Changes in Tmax under RCP 2.6, 4.5, 8.5 Scenarios with two sub-models.

	SDSM-A			SDSM-M		
	RCP2.6			RCP2.6		
	2020	2050	2080	2020	2050	2080
Summer	0.10	0.07	0.08	-7.07	-3.96	-4.19
Spring	1.07	1.30	1.62	-7.55	2.83	2.38
Autumn	0.37	0.22	-0.01	-9.57	0.81	0.22
Winter	4.18	4.23	4.18	-7.49	6.40	5.62
Annual	1.03	1.05	1.09	-8.13	-1.06	-1.56
	RCP4.5			RCP4.5		
Summer	0.10	0.09	0.11	0.11	0.09	0.10
Spring	4.60	4.51	4.49	1.19	1.21	1.22
Autumn	2.93	2.74	2.45	0.95	0.86	0.72
Winter	1.37	1.16	1.93	3.99	3.96	3.94
Annual	-1.18	-1.30	-1.42	1.04	1.02	1.00
	RCP8.5			RCP8.5		
Summer	0.17	0.12	0.14	0.08	0.05	0.06
Spring	2.73	2.93	3.19	1.18	1.14	1.11
Autumn	1.99	1.78	1.53	0.92	0.89	0.77
Winter	1.50	1.38	1.23	3.97	3.93	3.90
Annual	0.77	0.70	0.64	1.02	0.99	0.96

The primary aim of this research was to assess the Statistical Downscale Model (SDSM), using CIMP5 (CanESM-2) for different RCPs (2.6, 4.5 and 8.5) considering future changes in the Precipitation, Tmax and Tmin over the drainage area. The PRP (partial correlation percentage) for the predictors with high predictands values was determined. The Surface airflow strength (p_f) was found to be the best predictor for both temperature and rainfall. There were two other super predictors, surface meridional velocity (p_v) and surface zonal velocity (p_u) for almost all weather stations in the south-west of the Himalayan region of the Jhelum River Drainage Area (JRDA) Pakistan. These predictors also articulated a somatic relationship with PPT, Tmax, and Tmin. SDSM-M produced better results compared to SDSM-A for

all IPCC scenarios and determined the different levels of biases in the downscaled data at different seasons using GCMs (Su *et al.*, 2017).

Projections of climatic variability are associated with multiple imminent uncertainties from different places. The uncertainties include (1) Variations in the climate at the local scale (2) future scenarios (3) GCM's resolution and (4) downscaling methods (Ouyang *et al.*, 2014). The projected precipitation by both models for the 2020s, 2050s, and 2080s is with reference to the baseline period under the IPCC scenarios (RCPs 2.6, 4.5, 8.5). Both models showed increasing precipitation trends from 35% to 70% in the 2020s, 2050s, and 2080s. SDSM-M showed better results compared to SDSM-A for the baseline data. SDSM-A predicted a decrease in the annual and seasonal T_{min} in the 2020s, 2050s, and 2080s, but the winter season foresaw an increase from 1.26 °C to 1.88 °C. At the beginning of the 21st century, SDSM-M revealed a 3.75°C increase in the T_{min} but showed a decline of 0.11 °C in the minimum temperature by the end of the century. Similarly, for all IPCC scenarios, both models predicted increment for T_{max}. RCP 2.6 under SDSM-M showed a decline in the temperature from -7 °C to -4.19 °C at the start of the century, but at the end of the century, the temperature showed an increase from 0.22 °C to 5.62 °C. Burhan *et al.* (2018) also carried out a similar analysis of PDFs. However, more GCMs and emission scenarios needed to be evaluated, with other statistical downscaling approaches by utilizing a reliable process of selection of GCMs. The credibility of statistical downscaling models in non-stationary climate (Salvi *et al.*, 2016).

Conclusions: (It's too much detailed concise it and write in paragraph form) SDSM was used to downscale the projection of PPT, T_{max} and T_{min} by using CanESM-2 under the IPCC scenarios of RCPs 2.6, 4.5 and 8.5 in the JRDA. In this study, two models of SDSM were developed and evaluated to establish the correlation between the large scale variable and local scale variance in connection with 11 years (2002-2012) data. The current framework works out a partial correlation percentage (PRP) in a respective manner within 46.50%, 46.06%, 35.96%, and 21.97%. The R² values for both SDSM-M and SDSM-A models were calculated for all three scenarios 2.6, 4.5, and 8.5 RCPs under CIMP5 (CanESM-2). R² precipitation values under all three RCP scenarios were found to be between 82%-88% in SDSM-M. R² for T_{min} and T_{max} fell between 69%-71% and 68%-74%, respectively. For the SDSM-A model, precipitation lied between 76.5%-80% for while T_{min} and T_{max} existed between 85%-92% and 89%-96%, respectively. Both models projected seasonal and annual increase in precipitation under RCPs 2.6, 4.5 and 8.5 from 13%-68%, 25%-69% and 13%-71% during the period 2020s-2080s, respectively. T_{min} in annual models under RCP 2.6 showed a decreasing trend from -0.91 °C to -1.89 °C, -0.20 °C to -1.46 °C and -0.87 °C to -1.90 °C. The temperature under

RCPs 2.6, 4.5 and 8.5 reflected a rising trend during the period 2020s-2080s from 0.04 °C to 3.75 °C, 1.02 °C to 2.62 °C and 1.03 °C to 2.60 °C for the monthly model. Moreover, an increasing trend was noticed in the case of T_{max} from 0.01 °C to 4.18 °C, 0.01 °C to 4.49 °C and 0.12 °C to 3.90 °C during the 2020s-2080s under all three RCPs scenarios. The results predicted that the region will be warmer and wetter compared during the period 2020 to the 2080s. SDSM-A showed a normal variation for observed data compared to SDSM-M. In general, SDSM-A provided good results for average seasonal and annual temperatures (T_{max} and T_{min}).

In nutshell, the above results revealed that JRDA is expected to experience more extreme events in the 21st century. To mitigate the impacts of these events on human life as well as economic and ecological stability, strong emphasis needs to be put on identifying the nature and extent of danger to be caused by these extreme events and then on acting accordingly. This research will be helpful for water resources planning under different climate change scenarios.

Acknowledgement: This study was assisted by the National Natural Science Foundation of the China (no. 51509141, 51809150) and China Scholarship Council.

Conflict of interest: None

REFERENCES

- Azmat, M., M.U. Qamar, S. Ahmed, M.A. Shahid, E. Hussain, S. Ahmad and R.A. Khushnood. 2018. Ensembling downscaling techniques and multiple GCMs to improve climate change predictions in cryosphere scarcely-gauged catchment. *Water Res. Manag.* 32:3155-3174.
- Akhtar, M., N. Ahmad and M.J. Booij. 2008. The impact of climate change on the water resources of Hindukush-Karakorum-Himalaya region under different glacier coverage scenarios. *J. Hyd.* 355:148-163.
- Ashiq, M., C. Zhao, J. Ni and M. Akhtar. 2010. GIS-based high-resolution spatial interpolation of precipitation in mountain-plain areas of Upper Pakistan for regional climate change impact studies. *Theo. Appli. Clim.* 99: 239-253.
- Borges, P.D.A., K. Barfus, H. Weiss and C. Bernhofer, 2017. Extended predictor screening, application and added value of statistical downscaling of a CMIP5 ensemble for single-site projections in Distrito Federal, Brazil. *In. J. ofClima.* 37:46-65.
- Byun, K. and A.F. Hamlet. 2018. Projected changes in future climate over the Midwest and Great Lakes region using downscaled CMIP5 Ensembles. *Int J Clim.* 38:531-553.
- Basha, G., P. Kishore, M. V. Ratnam, A. Jayaraman, A. A. Kouchak, T. B. Ouarda, and I. Velicogna. 2017.

- Historical and Projected Surface Temperature over India during the 20th and 21st century. *Sci. Rep.* 7:1-10.
- Burhan, A. 2018. The analysis of climate change in Pakistan. ISBN: 978-613-8-51281-3.
- Chu, J., J. Xia, C.Y. Xu and V. Singh. 2010. Statistical downscaling of daily mean temperature, pan evaporation and precipitation for climate change scenarios in Haihe River, China. *Theo. & App. Clima.* 99:49-161.
- Fowler, H.J., S. Blenkinsop and C. Tebaldi. 2007. Linking climate change modelling to impacts studies: recent advances in downscaling techniques for hydrological modelling. *Int. J. of Clima.* 27:1547-1578.
- Huang, J., J. Zhang, Z. Zhang, C. Xu, B. Wang and J. Yao. 2011. Estimation of future precipitation change in the Yangtze River basin by using statistical downscaling method. *Stoc. Env. Res. & Risk Asses.* 25:781-792.
- IPCC. 2013. The physical science basis. In: Contribution of working group I to the fifth assessment report of the intergovernmental panel on climate change. Intergovernmental Panel on Climate.
- IPCC. 2007. The physical science basis. In: Solomon S, Qin D, Manning M, Chen Z, Marquis M, Averyt KB, Tignor M, Miller HL (eds) Contribution of Working Group I to the fourth assessment report of the intergovernmental panel on climate change. Cambridge University Press, Cambridge.
- Khan, M.S., P. Coulibaly and Y. Dibike. 2006. Uncertainty analysis of statistical downscaling methods. *J. of Hydr.* 319:357-382.
- Lowry A.M., P.R. Pearce, C. Barkus, S.J. Anderson, and J.A. Clement, 2017. Auckland region climate change projections and impacts: summary report. National Institute of Water and Atmospheric Research.
- Liu, J., J.R. Williams, X. Wang and H. Yang. 2009. Using MODAWEC to generate daily weather data for the EPIC model. *Envi. Mod. & Sof.* 24:655-664.
- Li Liu, D., G. J. O'leary, B. Christy, I. Macadam, B. Wang, M. R. Anwar and A. Weeks, 2017. Effects of different climate downscaling methods on the assessment of climate change impacts on wheat cropping systems. *Clim. Chan.* 144:687-701.
- Masson, V., C. Marchadier, L. Adolphe, R. Aguejdad, P. Avner, M. Bonhomme, G. Bretagne, X. Briottet, B. Bueno, C. de Munck, O. Doukari, S. Hallegatte, J. Hidalgo, T. Houet, L. Bras, A. Lemonsu, N. Long, M.P. Moine, T. Morel, L. Nologues, G. Pigeon, J.L. Salagnac, V. Vigié and K. Zibouche. 2014. Adapting cities to climate change: a systemic modelling approach. *U. Clim.* 10:407-429.
- MEb. 2018. Climate change projections for New Zealand: atmosphere projections based on simulations from the IPCC fifth assessment, 2nd edn. Ministry for the Environment, Wellington.
- Ouyang F, H. Lu, Y. Zhu, J. Zhang, Z. Yu, X. Chen and M. Li. 2014. Uncertainty analysis of downscaling methods in assessing the influence of climate change on hydrology. *Stoch Env. Res. Risk. Assess.* 28:991-1010.
- Rummukainen, M. 2010. State-of-the-art with regional climate models. *Rev. Clim. Change.*, 1:82-96.
- Salvi, K., S. Ghosh, and A. R. Ganguly, 2016. Credibility of statistical downscaling under nonstationary climate. *Clim. Dyn.* 46:1991-2023.
- Su, H., Z. Xiong, X. Yan, X. Dai and W. Wei. 2017. Comparison of monthly rainfall generated from dynamical and statistical downscaling methods: a case study of the Heihe River Basin in China. *Theo. App. Clima.* 129:437-444.
- Su, B., H. Jinlong, G. Marco, J. Dongnan, T. Hui, T. Jiang, and Z. Chengyi. 2016. Statistical downscaling of CMIP5 multi-model ensemble for projected changes of climate in the Indus River Basin. *Atmos. Res.* 178:138-149.
- Wilby, R.L., 2007. A review of climate change impacts on the built environment. *Built. Environ.* 33:31-45
- Wilby, R. and C. Dawson, 2007. SDSM 4.2 a decision support tool for the assessment of regional climate change impacts, user manual. Department of Geography, Lancaster University, Lancashire.
- Wilby, R.L., C.W. Dawson and E.M. Barrow, 2002. SDSM—a decision support tool for the assessment of regional climate change impacts. *Envi. Mod. Soft.* 2:145-157.
- Zhao, P., H. Lu, H. Yang, W. Wang and G. Fu. 2019. Impacts of climate change on hydrological droughts at basin scale: a case study of the Weihe River Basin, *Quat. Inter.* 513:37-46.
- Zaman, M., S. Yuan, J. Liu, M. Usman, I. Ahmad, F.A. Chandio, M. Saifullah, M.U. Liaqat and M. Adnan, 2017. Quantifying the Effect of Climate Change on Precipitation and Temperature Patterns by Using Variant of Non-Parametric Techniques. *Fres. Envi. Bull.* 26:7419.
- Zaman, M., G. Fang, M. Saifullah and Q. Javed, 2016. Seasonal and Annual Precipitation Tren.

[Received 25 Oct 2019; Accepted 20 April 2020; Published (online) 08 June 2020]